ACTA NEUROBIOLOGIAE EXPERIMENTALIS

Acta Neurobiol. Exp. 1996, 56: 927-942

Nonlinearities within the cat LGN cell receptive fields in simulated network with recurrent inhibition

Paweł Musiał[1], **Stanisław Panecki**[1], **George L. Gerstein**[2] and **Andrzej Wróbel**[3]

[1,3]Department of Neurophysiology, Nencki Institute of Experimental Biology, 3 Pasteur St., 02-093 Warsaw, Poland,
Email: wrobel@nencki.gov.pl; [2]Department of Neuroscience, University of Pennsylvania, Philadelphia, PA 19104-6085, USA

Abstract. We investigated the receptive fields of principal cells from the cat's lateral geniculate nucleus cells. About 20% of the X type neurones showed clear nonlinearities of summation when stimulated by two simultaneously onset, small bars of light. The possible source of this nonlinearity was studied on a specially designed model of a one-layer neuronal network with inhibitory, recurrent interactions, intended to mimic the inhibitory influence exerted on geniculate relay cells by perigeniculate interneurones. The model, when activated from periphery by two stimuli-like input patterns, produced at the output side the nonsymmetrical profiles of the receptive fields sensitivity, similar to those obtained in real experiments. This nonlinear output appeared when some of the relay cells were inhibited below their firing level threshold and this effect was spread through the network by lateral inhibitory connections. It is concluded that physiologically observed nonlinearities of the order of single receptive field mechanisms can be predicted by a simple recurrent network.

[3] To whom correspondence should be addressed

Key words: nonlinear properties of the receptive fields, X cells, recurrent inhibition, one-layer model

INTRODUCTION

Neuronal network of the LGN principal cells

The visual analyzer of mammals is, at its lower levels, one of the best described systems in the brain and therefore sets a good chance for physiological modelling. Its thalamic part, investigated in this experiment, starts with the ganglion cell axons which excite the lateral geniculate nucleus (LGN) principal cells and intrageniculate interneurones. Intrageniculate interneurones *via* their feed-forward connections inhibit in turn the principal cells. Axons of LGN principal cells, projecting to the visual cortex, give off collaterals to the perigeniculate nucleus (PGN) which consists exclusively of GABA-ergic interneurones. PGN neurones inhibit the geniculate principal cells by their recurrently projecting axons.

Each LGN principal cell is inhibited by up to 7-8 intrageniculate feed-forward interneurones and many recurrent PGN neurones (Lindström 1982). The intrageniculate interneurone receives inputs from one to a few neighbouring retinal ganglion cells and inhibits further a few principal neurones. Similarly, each perigeniculate interneurone receives excitatory input from at least 16 neighbouring (in a retinotopic sense) principal cells from the LGN (Ahlsen et al. 1983) and exerts recurrent inhibitory action on many other cells in this nucleus (Ahlsen et al. 1985, Sherman and Koch 1986). The LGN-PGN recurrent loop diverges more than the retino-thalamic pathway but, in general, preserves its retinotopic organization.

All of the thalamic cells involved in the above circuitry (principal cells as well as both types of interneurones) receive excitatory input from the cortico-thalamic fibres (Tsumoto at al. 1978, Lindström and Wróbel 1990). Additionally, all of these cells are under different modulatory actions from the lower parts of the brain (see McCormick 1992, for a review). The external inputs provide an important conditions for physiology of the LGN during visual behaviour. Their role, however, seems to be limited to modulation of the fundamental mechanism of the nucleus which appears to be based on the circuitry providing lateral inhibition (Hubel and Wiesel 1961, Ahlsen et al. 1985).

Properties of LGN RFs

The structure and function of a cell in the visual system is usually described by its receptive field (RF). The RF is delineated as such a part of a retina, stimulation of which changes activity of a cell under investigation.

The receptive fields of LGN principal cells and intrageniculate interneurones are organized in a similar fashion as the retinal ganglion cells RFs (Hubel and Wiesel 1961, Cleland et al. 1971, Hoffman et al. 1972, Dubin and Cleland 1977, So and Shapley 1979, 1981, Lehmkuhle et al. 1980, Troy 1982, Wróbel 1981, 1982, Wróbel and Tarnecki 1984). The receptive field of a principal cell when measured by its extracellular activity has a circular symmetry with a central excitatory zone and inhibitory surround. The opposite phase stimulation results in antagonistic responses (Fig. 2A).

The two types of LGN cells' receptive fields are ON- and OFF-centre. ON-centre cell increases its activity in reaction to the onset of light stimulus on dark background in the RF centre and decreases activity after stimulus in that region is switched off. The onset of light stimulus in the surround reduces the firing rate of ON neurone, its offset - enhances cell activity. The OFF-centre neurones respond with the same pattern for dark stimuli on light background. Still other classification of geniculate neurones is based on the summation process taking place within their RFs. It has been shown that both ganglion cell (Enroth-Cugel and Robson 1966) and LGN neurones can exhibit either linear or nonlinear summation of the excitatory and inhibitory inputs activated during stimulation of theirs RFs (Cleland et al. 1971, So and Shapley 1979). The corresponding neurones are called X- and Y-type. These two neuronal types can belong to either ON- or OFF-centre class.

The RFs of LGN principal cells differ from those of the retinal ganglion cell neurones only by their

enhanced centre-surround antagonism. The additional inhibition is due to the lateral connections at the geniculate level (Hubel and Wiesel 1961). This lateral inhibition is composed by two types of inhibitory interneurones described above. The intrageniculate interneurone provides feed-forward inhibition of the same type as centre response of the cell (e.g. ON-inhibition in ON-centre cell, Lindström and Wróbel 1986). Perigeniculate recurrent inhibitory cells have ON-OFF type receptive fields and therefore exert both types of inhibition on the LGN principal cells (Dubin and Cleland 1977, Lindström and Wróbel 1986).

Receptive fields of the perigeniculate interneurones are at least twice as big in diameter as those of LGN principal cells and they are lacking the characteristic centre-surround arrangement (Dubin and Cleland 1977, So and Shapley 1981, Ahlsen et al. 1983, Wróbel and Tarnecki 1984). PGN interneurones respond also to stimulation of both retinas in contrast to principal cells and intrageniculate interneurones which have only monocular inputs. Such RFs arrangement suggests, that within the LGN, neurones of both ON and OFF types coming from the two eyes form morphologically separated visual pathways. These pathways converge not earlier than on the level of perigeniculate nucleus. In contrast, X and Y channels characterized on the retinal ganglion cell level are separated also within LGN and PGN neuronal populations.

The present experiment was set up in order to determine if complex visual stimuli (build up from two light-spots used typically for RF testing) are processed by the LGN as a sum of independent small stimuli or rather as an undivided entity, in a nonlinear fashion. The paper consists of two parts. In the first, we reveal the nonlinear properties of cell responses at the lateral geniculate nucleus (LGN). In the second part, we apply a simple model which mimics lateral inhibition with use of a recurrent pathway, to check if our understanding of information processing taking place at the LGN level is sufficient for modelling such physiological phenomena.

METHODS

Recording of physiological data

The physiological experiment was carried out on 21 adult cats and the main part of the data analysis has been reported previously (Wróbel and Gerstein 1979, Wróbel 1982). Seventy four cells were recorded for at least 6 h to get the whole experimental protocol completed. In this paper we refer to the subpopulation of X type LGN cells, which were shown to receive linear input from retinal ganglion cells (So and Shapley 1979). The detailed experimental procedure was described elsewhere (Stevens and Gerstein 1976). Shortly, after initial surgery, during which all possible sources of pain were removed, animals were placed in the stereotactic device, flaxedilized, artificially ventilated and kept during recording session on carefully administered local anaesthetics. The CO_2 and blood pressure were continuously monitored to evaluate the physiological state of the animals. Pupils were fully dilated with atropine, and corneas protected by contact lenses with artificial 6 mm aperture. Refraction was corrected by additional lenses in front of the eyes. After the experiment the animals were killed by overdoses of sodium thiopental (Nembutal) and their brains fixed and removed for further histological verification.

The single cells were recorded extracellularly by tungsten in glass microelectrodes and their spike activity window-triggered and registered by PDP-12 computer. Stimuli were small bars of light (0.25^{o} x 0.75^{o}) of 5 cd/m^2 luminance, projected on a tangent screen 1.2 m before the cat's eyes. The cells receptive fields were analyzed by building up the response and contour planes (Stevens and Gerstein 1976). The response plane is a stereoscopic view of subsequent post-stimulus time histograms obtained "simultaneously" for cyclic stimulation of succeeding separate 27 points spread over the RF axis by a small testing bar (Fig. 2A in the middle). The contour plane is a cut of response plane at the chosen firing level of the cell, projected on the spatiotemporal plane as shown in the right part of Fig. 2.

Structure, function and biological constraints of the model

The model has been implemented in the computer program written in Turbo Pascal and run on IBM-like personal computer (Panecki 1990). All simulations reported here were run with 16-bit accuracy of calculations and one simulation took about 20 min.

Simulated network is a one-layer set of 30x30 neurones interacting by means of lateral inhibitory connections. Each cell receives an external excitatory input and an inhibitory contribution from 8 adjacent neurones and itself (Fig. 1A). Activity of the model cell is a function of time and reflects mean firing rate of a real neurone. Input value X is transformed - according to a response function Λ- to the output Y. Input X corresponds to the postsynaptic potential in an axon hillock of a real neurone and Y - to the mean spike firing rate. The response function in our model is a linear function with a zero threshold:

$$Y = \Lambda(X) = \begin{cases} 0 & \text{for } X < 0 \\ const \cdot X & \text{for } X \geq 0 \end{cases} \qquad (1)$$

The frequency of firing of a real neurone is limited by its refractory period. Accordingly, we considered only those inputs that were sufficiently far from saturation range of the response function. By setting threshold of response function at zero we assumed that the cells reacted for each positive input. The input to the cell *i* consists of an excitatory part E_i and an inhibitory component coming recurrently from neighbouring cells and itself (Fig. 1A). The inhibitory input from the *j*th to the *i*th neurone is proportional to *j* cell activity and equals $-W_{ji}Y_j$, where W_{ji} is an absolute efficacy of the given inhibitory synaptic junction.

The model operates in a discrete time, measured in consecutive steps. The total input to *i* cell (X_i), is equal to external input minus all contributions from inhibitory cells. In the *t*-th step we get:

$$X_i = E_i(t) - \sum_{j \in S_i} W_{ji} \cdot Y_j(t-1) \qquad (2)$$

where S_i is a set of cells that inhibit the *i*-th one.

Inhibitory interactions are limited in our model to the recurrent inhibition as received by real LGN neurones from the PGN cells. The formula $-W_{ij}Y_j(t-1)$ corresponds to gross inhibitory effect of *j* cell on cell *i* by intermediate PGN interneurones action. The recurrent pathway includes also the investigated principal cell as probably is the case of a real network (Lindström and Wróbel 1986, Sherman and Koch 1986). We assumed that the feed-forward inhibition provided by the intrageniculate interneurones can be included by appropriate modification of spatial pattern of the external input (X) to the network (see also the Results section). Since the physiological experiment was carried out on the an-

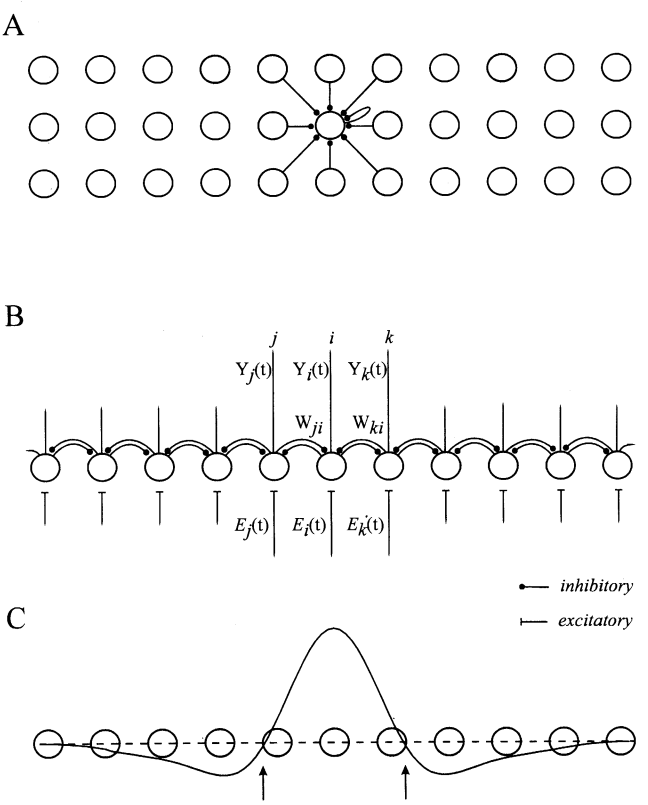

Fig. 1. A, overhead view of the part of neuronal network representing the LGN principal cells. All recurrent inhibitory connections are presented for one cell; B, lateral inhibition at the LGN level as modeled by one-layer network presented in this paper. E(t), Y(t) - input and output activity simulated in the model; C, "mexican hat": the shape of summed input activity to principal cell layer. It equals the retinal excitation lowered by lateral inhibition of feed-forward type as mediated in reality by intrageniculate interneurones.

aesthetized animals in which the excitatory corticothalamic projection was inactive (Hubel and Wiesel 1981), there was no need to include the cortical recurrent loop into the model.

The following expression describes activity of cell i of the model as a function of time:

$$Y_i(t) = \Lambda\left(E_i(t) - \sum_{j \in S_i} W_{ji} \cdot Y_j(t-1)\right) \qquad (3)$$

The model cells are positioned in nodes of a square net (Fig. 1A). We set the spatial scale in the model in such a way that the shortest distance between two cells equals 1. In order to avoid problems with border effects we provided inhibitory interactions between the first and last row as well as the first and last column of the network. All the cells have the same characteristics: the same response function and zero threshold. We also assumed symmetrical interactions between cells. This led to the following simplifications of inhibition strength as a function of distance and direction:

- symmetry of inhibitory interactions: interacting cells inhibit each other with equal strength;
- isotropy of inhibition: each cell is inhibited by its neighbours with the same strength regardless of the direction of the connection; within the inhibitory field the strength of inhibition does not depend on distance between cells. In reality inhibitory influence is mediated by more than one interneurone and number of synapses inhibiting a given cell should decrease gradually with the distance. A more realistic approach would yield only smoother decay of inhibition strength with a distance between cells.

As mentioned above, the activity in our model is expressed by the mean firing rate as a continuous function and measured in discrete time periods. The effects of input signals as well as inhibitory interactions from neighbouring cells incoming to the cell within one step interval are summed and treated as simultaneous. The model network state is updated in a random and asynchronous fashion. This means that the process of evolution for the whole network proceeds with consecutive random selection of a single cell which activity is then individually updated due to the current network state (Amit 1989).

RESULTS

Nonlinearities observed in the physiological data

We registered the activity of 21 ON-centre LGN principal cells, classified from their response plane as being of the X-type according to criteria given earlier (Stevens and Gerstein 1976). We stimulated the RF of the cell with two small stimuli presented in separate locations of the RF to obtain their response planes. The software allowed for simultaneous building of two separate response planes:

- first, when RF was stimulated along its axis by a single testing stimulus T (a small bar of light) (Fig. 2B).
- second, registered with synchronous presentation of stimulus T and additional conditioning stimulus (C) flashed in a fixed location on the RF axis.

The procedure was repeated for three different positions of C stimulus: in the centre of RF and in two symmetric locations on the border between centre and surround of RF, thus producing three sets of response planes, as presented in Fig. 2C.

Four ON-centre, X type neurones showed asymmetric responses (with respect to the RF centre) for simultaneously presented T and C stimuli, when C stimulus was located in either border between the RF centre and surround. The asymmetry in response was best observed in the surround of the RF (Fig. 2C). During on-phase of the stimulation it appeared usually as slight decrease of probability of firing (compared to the control plane presented in Fig. 2B) when C and T stimuli were on the opposite sides of RF centre, and increase of the cell's reaction when both stimuli were placed on the same flank of the field. These effects can be traced in the Fig. 2C as the "deeper" surround inhibitory domain evoked by double stimulation of the opposite flanks of the field and "blurring" of the same domain, when stimuli were placed on the same side of the field centre. If the summation mechanism was linear the observed responses would be symmetric with respect to the RF centre, as a sum of symmetric response for T

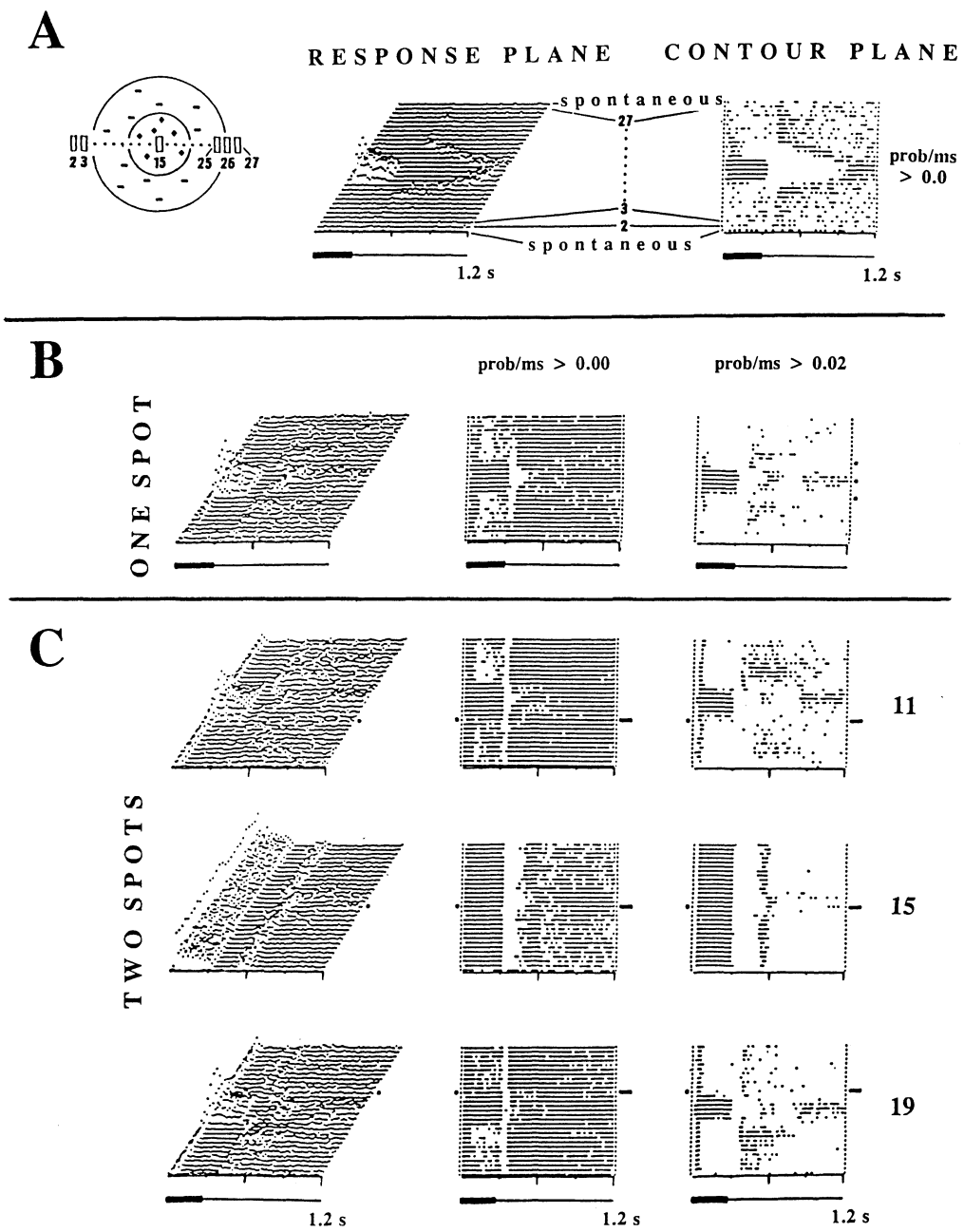

Fig. 2. A, left: the classic plot of the ON-centre LGN principal cell RF with 29 points of stimulation along the RF axis. Stimulus: 1^{o}x0.5^{o} bar of light of 5 cd/m^2 luminance. Middle and right: response plane and contour plane of the RF. B, responses of the ON-centre LGN principal cell of an X type, tested with single, T-testing spot. C, the same cell; simultaneously recorded response planes obtained with pair of stimuli: a T-spot and an additional C-conditioning stimulus, placed in the RF centre (position 15) or periphery (positions 11 and 19 out of 27) and switched on and off together with a testing one. The horizontal axis - time. Thick, black bar under the planes represent 330 ms of an on-time of stimulation. The thin line - 980 ms duration of off-phase. The ordinate represents the RF axis with 29 histograms recorded in 29 positions of the RF axis as shown in A. The two contour planes in B and C are cuts of the response planes correspondingly at the zero (middle column), and spontaneous probability of firing (most-right column) levels. The Z-axis in response planes represent no of spikes per bin. Bin width 20 ms. See text for further details.

stimuli and response pattern for C stimuli in a fixed location.

We have restricted the modelling to the X-type of LGN principal cells. This preselection was caused by the fact that Y-type channel exhibit nonlinearity already at the ganglion cell level (Enroth-Cugel and Robson 1966). Accordingly, among the recorded Y-type of LGN cells we have found the nonlinear summation phenomena of different type within 60% of the investigated sample (25 out of 43 neurones).

Modelling of the input function

While comparing the experimental results with the model simulation we omitted the temporal dynamics of the network. This was caused by the fact that short-time phenomena could not be reliably reflected by the activity of the model because of its discrete time sampling and relatively big time scale of a single step of simulation (which allowed for simultaneous summing all of inputs to a model cell). From these reasons we took for analysis only stable-states achieved by the network after several steps of evolution evoked by stationary input pattern (compare also the reasoning presented on the end of Results). The simulations were calculated only for the on-phase of stimulation, for the ON-centre cells.

As mentioned in the Introduction, firing of the principal cell depends on its excitatory input from the retinal ganglion cell axon modified by inhibition coming from the feed-forward interneurones. Such an input pattern of activity reaches LGN principal cell as a result of testing stimulus presented in consecutive steps along its RF axis. We modelled this pattern with a shape of typical "mexican hat" sampled in nodes of the network (Fig. 1C).

This shape was generated with the following function M which describes the spatial aspect of input activity:

$$M := A_1 \exp\left(-\frac{(r-r_0)^2}{b_1^2}\right) - A_2 \exp\left(-\frac{(r-r_0)^2}{b_2^2}\right)$$

while $A_1 > A_2$, $b_1 < b_2$

where r_0 - position of the pattern maximum; if r_0 indicates location of a particular cell it means that the point stimulus is presented on the RF centre of this cell.

The above description is based on the Rodieck-Stone model of receptive field sensitivity of retinal ganglion cell (Rodieck and Stone 1965). In their model the response of a ganglion cell is formed by two mechanisms: strong, excitatory called the central mechanism and weak, inhibitory - peripheral mechanism. Both of them culminate in the field centre but the strength of excitatory mechanism decreases faster than inhibitory. In effect, the excitatory mechanism predominates in the RF centre and the inhibitory one - in the surround.

Since the feed-forward inhibition, added by intrageniculate interneurones, is also the strongest in the field centre (Lindström and Wróbel 1986) and influences the principal cell at its input site, it can be included together with retinal input into one inhibitory component of M function.

Even a small stimulus, as used in our experiment, affects more than one retinal ganglion cell. This results from spatial overlap of neighbouring retinal ganglion cells' RFs. This overlap is defined by the coverage factor (CF), a proportion of total area of RF centres covering a given region to the area of that region. The CF in a given point of the retina may be expressed by an average number of cells excited by the point-stimulus presented to this site. The coverage factor for the ON centre X cells was experimentally found to be about 3.5 - 10 (Peichl and Wässle 1979). The overlap of the retinal RFs blurs the activity pattern at the input to LGN. This was presented in the function M by wider central mechanism which includes a few neighbouring retinal fibres (Fig. 1C). For the sake of the above presentation, we assumed that each LGN principal cell receives its input from only one corresponding retinal ganglion cell. Although it is true for only about 60% of X neurones recorded in LGN (Levick et al. 1972, Wróbel and Lindström, unpublished results) the resulting convergence is not crucial for our analysis and can be included together with the coverage factor parameter.

The spatial activity pattern M at the input to LGN-network was finally modelled as equal to the

global retinal output decreased by intrageniculate inhibition. In the further text, we shall consequently refer to this pattern as a "mexican hat" stimulating the geniculate network. Its spatial extent is described by the distance where both mechanisms: excitatory and inhibitory, have equal strength (arrows in Fig. 1C). This distance can be evaluated on the response plane of principal neurone as a central excitatory domain measured at spontaneous activity level (Fig. 2B).

All sources of spontaneous activity of principal neurones (intrinsic background, pontine and cortical inputs) are included into the model as a homogenous component B imposed on the main external input pattern M as:

$$E = M + B$$

Every principal neurone was modeled to be inhibited by 9 recurrent connections which originate from its nearest neighbours and from itself (Fig. 1A). The diameter of the effective recurrent inhibitory surround of the RF of LGN principal neurone is twice as big as the field centre. This size was estimated during physiological experiments by measuring the opposite phase inhibition (OFF inhibition in ON-centre cell). The only source of such inhibition can be the PGN cells since the intrageniculate interneurones yield inhibition of only the same phase as the central response (Lindström and Wróbel 1986).

We assumed that summation of responses within the retinal receptive fields is linear (to fulfil this criterion, we restricted our model to X-type cells as discussed above). With such assumption, simultaneous presentation of two stimuli on the retina is equivalent to LGN input obtained by summation of two appropriate "mexican hat" activation functions and the homogenous background.

Simulation of the electrophysiological experiment

We simulated both parts of the physiological experiment (Figs. 2B and C) using the model presented above. Although simulations were carried out in a 2-dimensional network, for clarity we limited presentation of results to one row of cells that corresponded to the receptive field axis of a selected cell *a*. This row of cells is represented by means of vertical ticks on the abscissa in Figs. 3A to D. The cell activities are represented along ordinate axis. Points representing activity of consecutive cells in the row are connected by a dotted line and form a plot of activity of the row of cells at given time of experiment. Plots corresponding to successive phases of simulation (e.g. consecutive T stimulus positions in Fig. 3A) are arranged along the depth axis. A perspective view of such plots represents the stable steady-states of the network calculated for consecutive stimulation arrangements.

Figure 3A mimics the physiological experiment shown in Fig. 2B. The testing stimulus (T), of a "mexican hat" shape (as shown in Fig. 1C), was centred in successive 101 positions (0,1,..,100) along the RF axis of cell *a*. In subsequent phases of simulation the T stimulus was located at $d/10$ distance to the right from position occupied in the previous phase (where d was a distance between model cells in the row). Thus the facing plot (marked 0 at the depth axis) corresponds to the activity of the row of cells evoked by T stimulus located at the distance $5d$ to the left from the selected *a* cell. The 50th plot corresponds to the activity of the same row of cells but with T stimulus centred at location *a*. Finally, the last plot (position 100) represents the activity of the same row of cells excited by T stimulus placed in position $5d$ to the right from *a*. For each stimulus position the stable steady state was achieved by the network after required time of evolution (20 steps). The thick continuous curve, parallel to the depth axis, represents the activity of the neurone *a* as stimulated by T stimulus located in consecutive positions (0 .. 50 .. 100) and corresponds to the RF sensitivity function measured during physiological experiment. The large black dot on this curve, corresponds to RF position (55) in which the C stimulus will be centred in experiment shown in Figs. 3B and C.

Figure 3C represents (with similar outline as Fig. 3A) the activity of the same chosen row of cells

when stimulated by conditioning stimulus C placed at the same position 55 throughout all 101 phases of simulation. This position was close to the centre/surround border of the RF sensitivity function of the cell *a* (dot on the thick continuous line in the Fig. 3A).

Figure 3B shows the response of the same row of cells to two simultaneously presented T and C stimuli, with T stimulus in successive 101 positions and C stimulus placed in a fixed position number 55. Accordingly, the thick continuous line represents the activity of the neurone *a* in subsequent phases of simulation.

Figure 3D shows the resulting nonlinearity of the network response in a magnified scale. The nonlinearity N was defined as a difference between the sum of responses to separately presented stimuli T and C, and the response to both simultaneously presented stimuli:

$$N = ([T]+[C]) - [T+C]$$

The difference between sum of responses of the cell *a* for separately applied T and C stimuli and combined T+C stimulus is shown as continuous thick line parallel to the depth axis in Fig. 3D and then repeated in Fig. 4. When stimulus C was presented at the right side of the RF centre (black triangle in Fig. 4) the resulting activation of a cell is lower than predicted by simple algebraic rule (the thin line to the left of the RF centre). The nonlinear net effect is shown in Fig. 4 as deviation from zero level (thick continuous line). The observed nonlinear effect of summation mimics well experimental

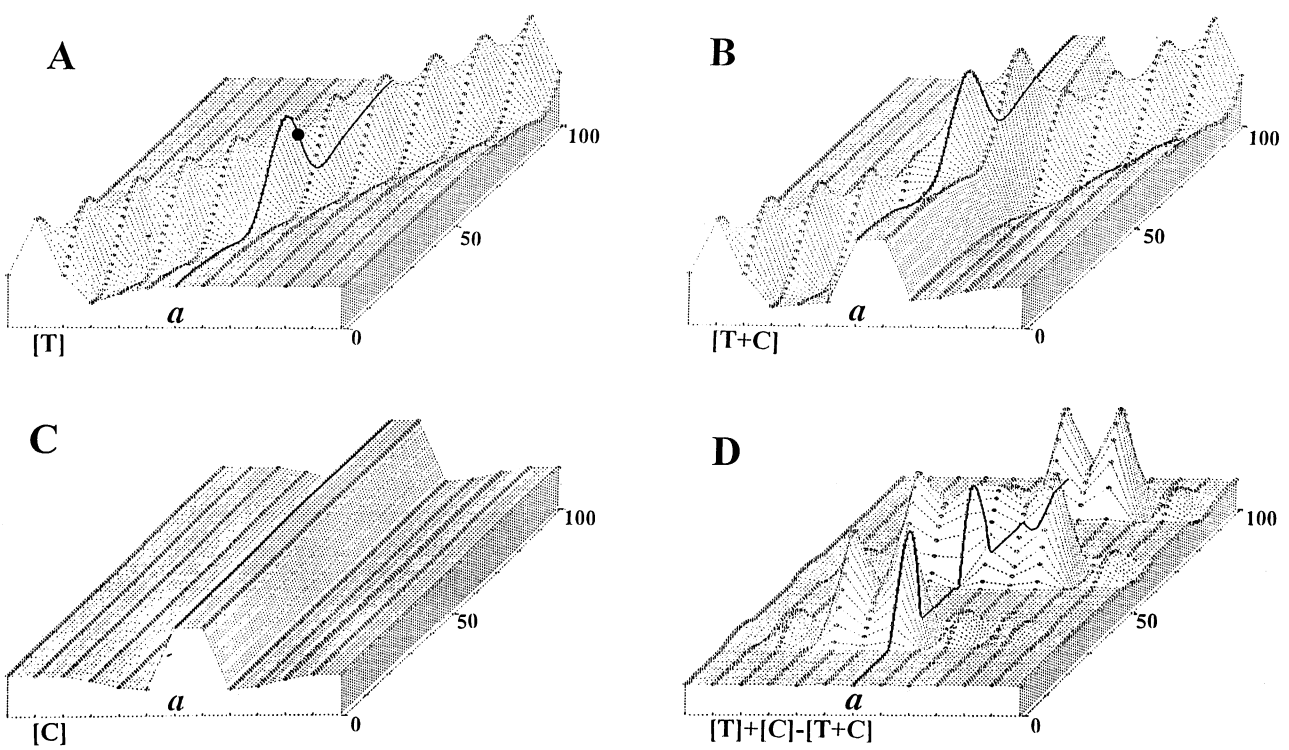

Fig. 3. A, responses of the selected row of cells for T stimulus. Numbers 0-100 indicate the position of maximum of M function at the input site. The sensitivity function of cell *a* is drawn by a thick line. Black dot on this line indicates the position in which C stimulus was located in next stages of the experiment (B,C,D); B, Responses of the same row of cells obtained after simultaneous stimulation with T and C stimuli. C, the same row of cells stimulated exclusively by conditioning stimulus C. D, nonlinearity measured as a difference of summed blocks of responses represented in A and C, and response block in B. Abscissa, distance along the given row of network; axis in depth, activity of the row of cells stimulated by stimulus T placed in all consecutive positions; the continuous curves represent the responses of *a* cell in consecutive simulations. See text for details.

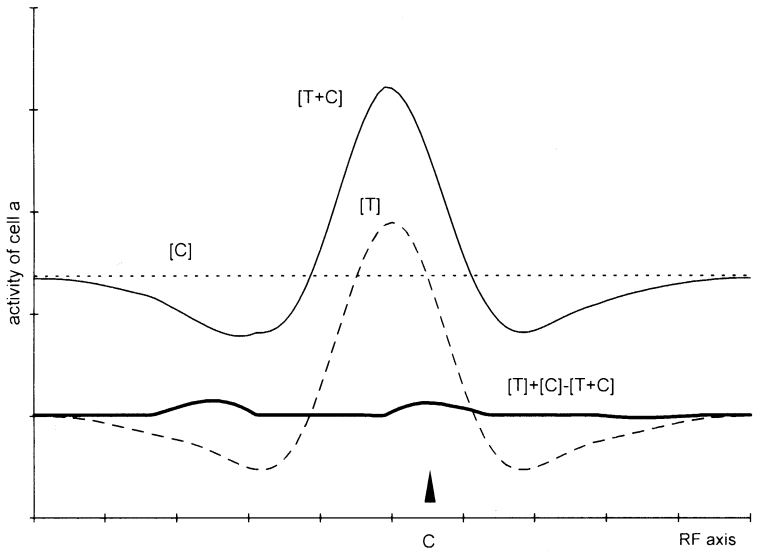

Fig. 4. The responses of the cell *a* in consecutive simulations performed with the testing spot applied in all 100 positions. The conditioning spot was applied always in a fixed position marked on the abscissa. The dashed line shows the *a* cell activity when it responded for a single testing stimulus in all positions (marked [T]). It corresponds to the thick line in Fig. 3A. The thin continuous line represents the responses of *a* cell in double stimuli experiment ([T+C]). It corresponds to the thick line in Fig. 3B. The dotted line represents the level of response of the cell *a* for C stimulus alone placed in position 55 ([C]). The thick continuous line represents the nonlinearity measured as difference between sum of responses for separate presentation of T and C stimuli and responses for simultaneous double stimulation ([T]+[C]-[T+C]).

results as obtained during physiological experiment presented in Fig. 2, for stimulus positions 11 and 19.

Note that the responses of the model cells in the central region of the field are about two times larger when RF is activated by two stimuli (continuous thin line in Fig. 4) as compared to testing stimulation alone (dashed line in Fig. 4). This effect is not observed in the real experiment, most probably, because of saturation of high frequency responses of LGN cell (above 300 Hz). Indeed, the two spots stimulating simultaneously the RF centre do not evoke prominently enhanced response during ON--phase (Fig. 2C, middle row).

The nonlinearity shown in Figs. 3 and 4 depends on the relative position of C and T stimuli. Nonlinearities for every combination of C and T stimuli positions are presented in Fig. 5. Figure 5A shows a 3-dimensional version of the upper part of the contour map shown in B.

The threshold effect was observed only for limited range of relative positions between stimuli T and C. The zero firing level could be reached only in such cases when surrounds of input firing patterns (represented by decrease of activity, comp. Fig. 1C) overlapped and summed. Such conditions could be fulfilled when two input patterns overlap almost completely or when two centres are apart and only surrounds overlap. This is the reason why nonlinearities shown in Fig. 5B appear only around the diagonal and why there are no nonlinearities in farther regions. The central diagonal in Fig. 5B corresponds to the first variant of input patterns arrangements and the two outer diagonals, to the second arrangement.

Properties of the model network nonlinearities

Our computations have shown that a simple network model with recurrent inhibition can yield a nonlinear output even with all processes on its input side being linear. This nonlinearity appears only when the sum of inputs applied to any of the cells in the network becomes negative. By cutting off negative signals the model changes the input values. This is the only possible source of nonlinear phenomena in our simulations. The additional "input" to silenced cells results in increased lateral inhibitory influence which they exert on their neighbours. The inhibited neighbours evoke disinhibition on yet further cells in the network. The resulting nonlinearity spreads over the network in form of concentric waves around the cells affected by threshold

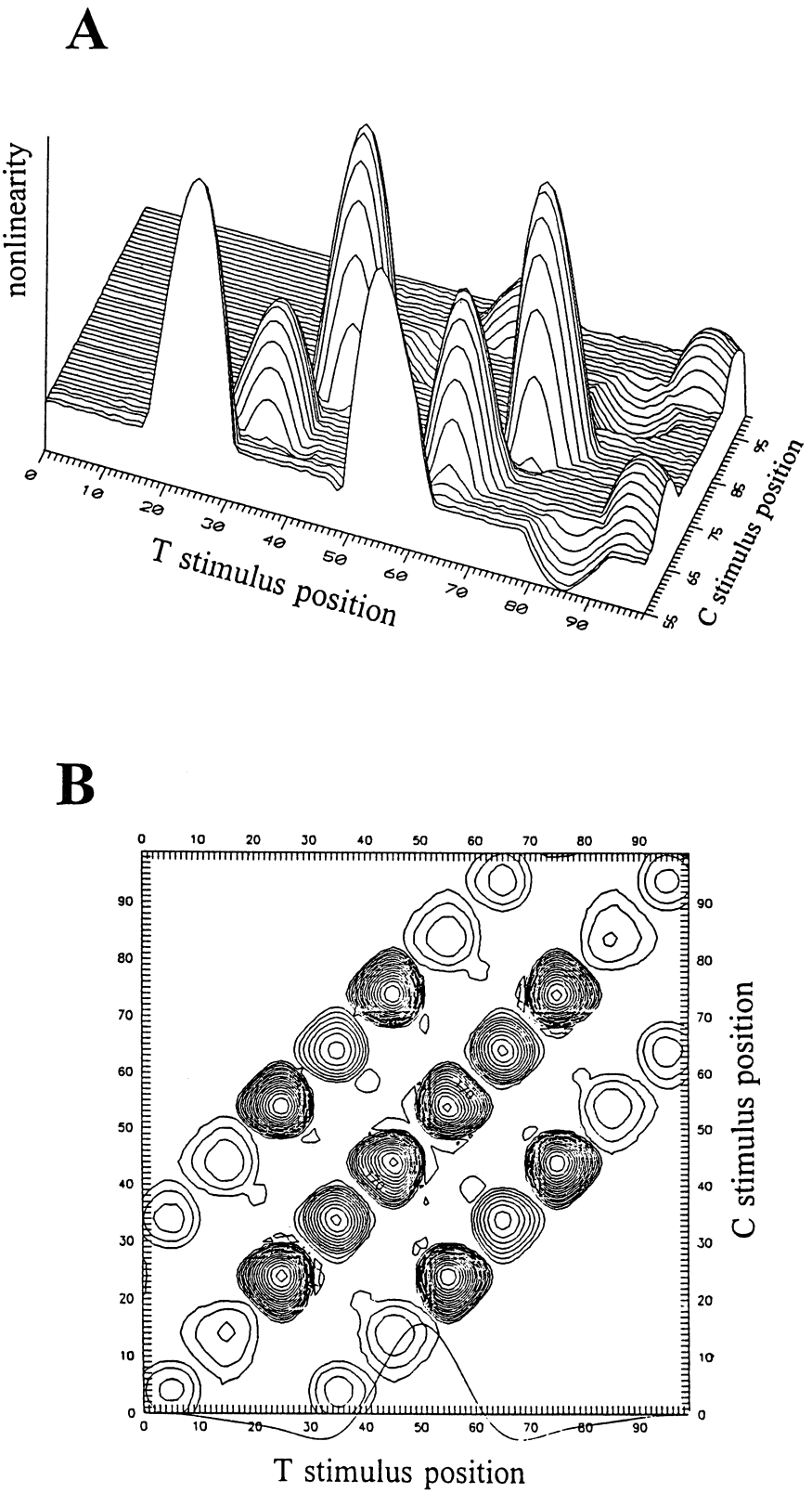

Fig. 5. A, nonlinearities of responses of cell *a* as simulated along its receptive field axis (testing spot position 1,2,..,100) for subsequent positions of conditioning stimulus 55,56,..,100; B, The contour map of nonlinearities of cell *a* responses for all locations of C (1,2,..,100) and T stimuli. On the abscissa axis the sensitivity curve of a RF of cell *a* is superimposed.

effect (compare the waves diminishing along the horizontal axis in Fig. 3D).

Figure 6A shows a limited fragment of the network, including the cell *a*, which was activated by simultaneous presentation of T and C stimuli. Two cells marked by black dots were strongly inhibited by the input pattern and set to zero activity level according to the threshold rule. They became the seed for the nonlinear effect to spread further over the network. The nonlinear effects in the row of cells including the cell *a*, can be better traced in Fig. 6B. Note, that the cell *a* which was located in the closest vicinity of the "source of nonlinearity" is less excited (Figs. 4 and 6B, at testing spot position T=25) than it would be in a fully linear model (without threshold setting as defined by physiological properties).

The threshold effect may appear when inhibitory surrounds from two "mexican hat" inputs overlap, as well as when strong lateral inhibitory effect originates from the large central excitation (Figs. 4 and 5B, for the testing spot T position = 55). Similar effects were observed also in physiological experiments. The inhibitory domains surrounding RF central domain response were enhanced on the flanks contralateral to applied conditioning stimulus C and weakened on the ipsilateral flanks (Fig. 2C).

The threshold rule leading to nullifying the negative activation values is equivalent to introducing an additional excitatory stimulus to the input side. As shown above, these extra excitatory inputs are actual sources of the observed nonlinearities. Thus, for visualizing the nonlinear influences within the network we studied the spread of excitation evoked by point stimulus on homogeneous background B (Figs. 7 and 8).

Network with the recurrent inhibition stimulated by a point stimulus manifests greater spatial extent of resulting activity than the actual size of the input

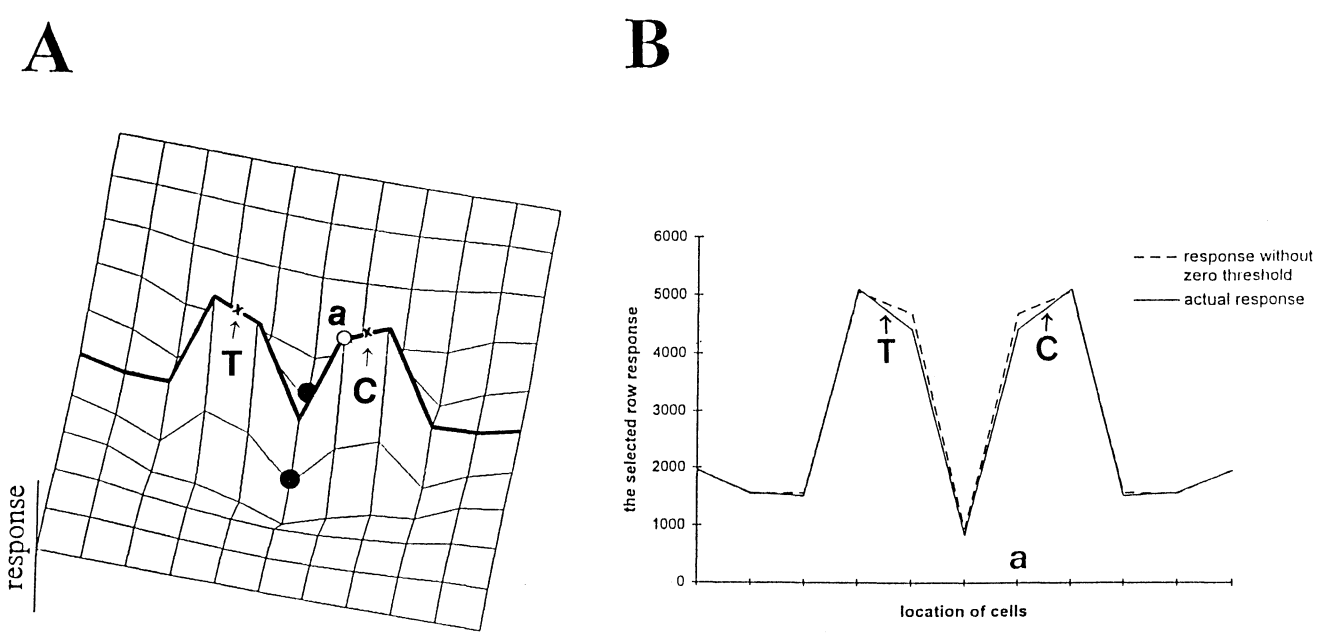

Fig. 6. A, perspective view of stabilized activation of the model network exerted by two stimuli placed along the selected row (thick line) in positions: 25 (T) and 55 (C) (both marked by crosses). The two cells which were silenced by inhibitory action are marked by black dots. The position of cell *a* is marked by open circle; B, continuous line represents the activity of row of cells marked in A by a thick line. The dashed line shows the sum of appropriate responses of the same row of cells as recorded after separate stimulation by both stimuli. This sum is equal to response of a fully linear network, i.e. without zero threshold. The differences between the curves express the nonlinearities produced in the network.

stimulus pattern. The extent of this activation exceeds, in fact, also the range of intrinsic inhibitory connections since the consecutive network reverberations spread spatially during the evolution. Figure 7 shows stable states of the network with different inhibitory field parameters reached in response to an excitatory point stimulus. It is clear that with sufficient strength of inhibition the network activation oscillates in the spatial domain. With the increased range of the inhibitory field the spatial period of this oscillation also increases. Moreover, with increasing strength of inhibition amplitudes of the spatial oscillations as well as the extent of propagation grow while the gross activity of cells decreases (Fig. 7). The propagation extent parameter P (defined as a greatest distance between cell stimulated by the point stimulus and cells with changed activity) reached by the final stable state, is shown in Fig. 8. As can be seen, the propagation parameter P grows steeper with increasing inhibitory range.

We have found that the resulting nonlinear phenomena exceed the range of inhibition produced by the applied stimulus. This provides an additional argument that nonlinearities originate from inhibition of recurrent type. In the case shown in Fig. 4, the nonlinear response of the *a* cell obtained after simultaneous stimulation by C stimulus placed in posi-

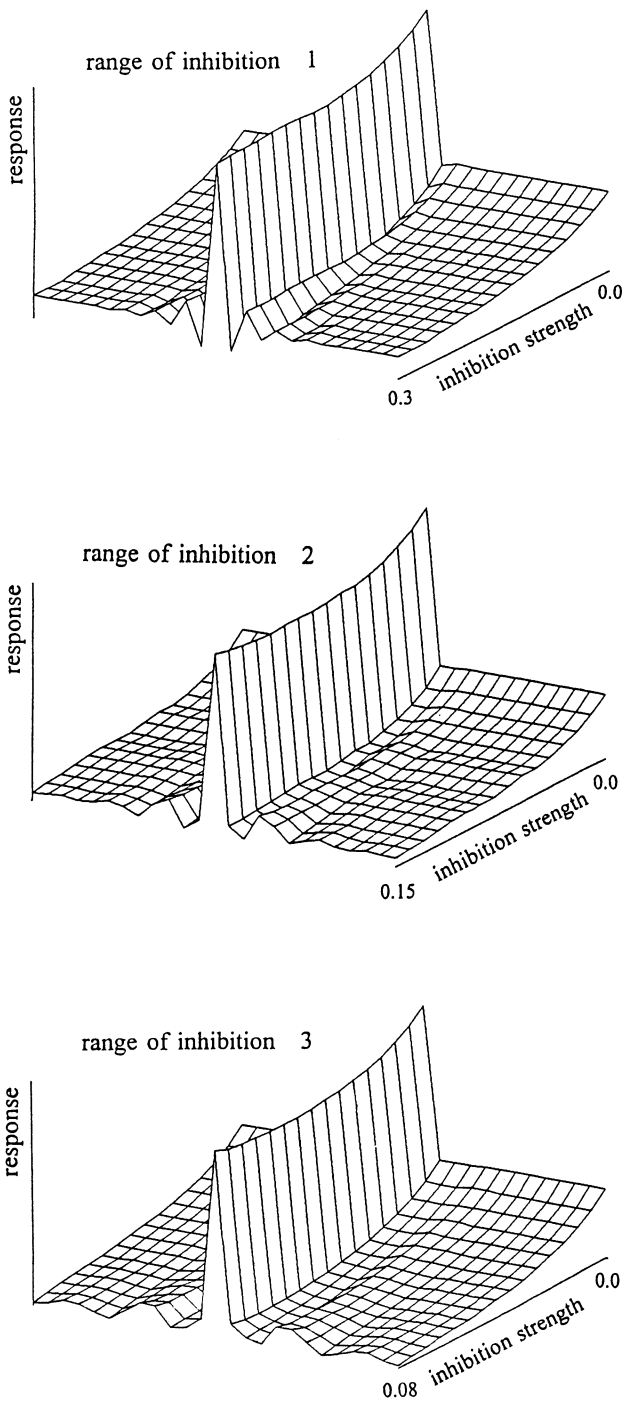

Fig. 7. The responses of cells from the selected row after stimulation exerted by a point stimulus and the homogenous background B. The two parameters studied are: strength and range of inhibition.

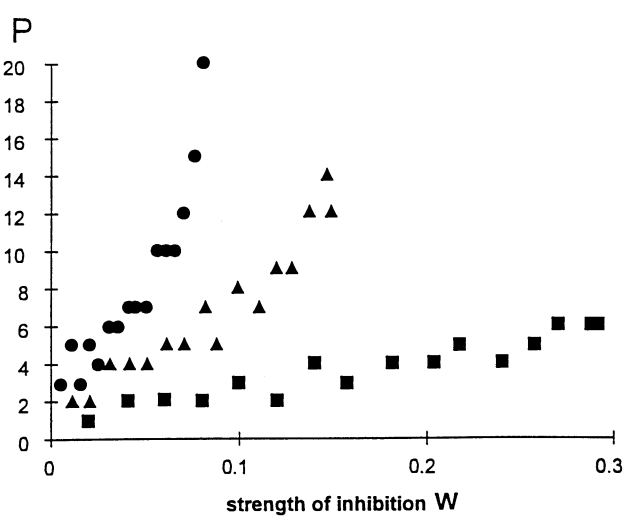

Fig. 8. The extent of activity propagation P as a function of range and W - strength of inhibition. Symbols: squares, for range of inhibition equal 1 (9 inhibiting cells, including inhibited one), triangles, for range of inhibition 2 (25) and circles, for 3 (49).

tion 55 and T - in 85, results from a threshold effect occurring in the cell that does not inhibit the *a* cell directly.

Further analysis showed that nonlinear effects decreased with growing radii of excitatory and inhibitory components (b_1 and b_2) of the used stimuli. These conclusion might be understood in view of following observations: (1) the amplitudes of the oscillations of network activity diminish rapidly with distance from their source; (2) the required overlap of inhibitory surrounds of larger "mexican hat" patterns, leading eventually to zero activity of some cells, appears in a larger distance from the cell *a*. The further the cell under observation is from the source of nonlinearity, the smaller is also the observed nonlinear effect.

Let us notice at the end, that all transient threshold effects, occurring during evolution and disappearing before the network reaches the steady stable state, do not contribute to the nonlinearities of the final response of the network. Let us consider the equilibrium state of the proposed network. During the time of further evolution response of any cell from the network should remain constant.

$$Y_{Ri} = \Lambda \left(E_i - \sum_{j \in S_i} W_{ji} \cdot Y_{Rj} \right)$$

for i= 1, ... ,N

where Y_{Ri} expresses the activity of cell *i* in the equilibrium state

As can be seen from the above set of equations the stable global network output can be fully expressed in terms of the input activation and the network parameters describing strength and spatial range of inhibition as well as the cell response function. The stable steady state does not depend on the initial or intermediate network states, for example by single cell updating order or by any nonlinear effects that may occur during the evolution.

DISCUSSION

In this paper we have been able to show that the nonlinear phenomena, observed in the responses of one fifth of our sample of X type ON-centre LGN cells, may be explained by simple threshold effect propagated by means of a recurrent inhibitory network. This effect occurs when some of the LGN cells are silenced by strong inhibition from summed surrounds of the incoming complex input stimuli (e.g. two spots). We do not deny that other nonlinear properties (of the cell or network origin) may contribute to the results obtained in our physiological experiment. Each more complicated model system, however, should inherit the nonlinear mechanism described in the present paper.

When studying this nonlinearity we have assumed that all processes before the input to the investigated LGN network may be taken as linear. This assumption is an obvious simplification. Although Enroth-Cugel and Robson (1966) demonstrated linear summation within the separately investigated central (C) and surround (S) signals of the retinal X receptive fields, they were not able to demonstrate that the interaction of these processes is also linear (i.e. that the S is algebraically subtracted from C). The simplification provided in this paper ensures that all nonlinear effects occurring during the simulations result only from the features of LGN and PGN neural network as discussed below. The 5 ON-centre optic tract fibres recorded as a control sample in this experiment did not show a trace of nonlinear effects as described in the Results for LGN principal cells. This supports the notions that the discussed nonlinearities may be intrinsic also to the real geniculate network.

The number of ganglion cells within the LGN which are excited by the point stimulus falling on retina (coverage factor CF, see Introduction) equals the number of overlapping centres of receptive field at the given point. Since the typical X-type relay cell in the LGN receives only one ganglion cell axon their coverage factor could be estimated as being of similar value. During the calculations, we searched for such an input stimulation pattern which would cause the largest nonlinear phenomena at the output side. This search resulted with the estimation of CF value between 4 and 9. According to Peichl and Wässle (1979) the real coverage factor for X-type retinal ON ganglion cell is 3.5 to 10. Thus our model

results agree surprisingly well with the experimental data.

In fact about 40% of the LGN principal cells receive convergent input from more than one retinal ganglion cell fibres (Wróbel and Lindström, unpublished results). When assuming more numerous retinal fibre divergence we would come up with wider input pattern and therefore smaller nonlinear effects (see above). At the same time, however, the larger spatial extent of inhibitory interactions between the model cells would widen spatial oscillations and expand the propagation factor P, both leading to larger and more extensive nonlinearities.

In the presented model we assumed that feed-forward type of inhibition could not lower the cell activity toward the firing threshold level. Most probably this was not a realistic assumption. In fact, the first order nonlinear phenomena found in this experiment could be also produced by strong inhibitory action of the feed-forward type. Were this type of inhibition allowed to stop the cell firing, its action would be limited to targeting cells. The more distant effects (comp. Fig. 8), should therefore be specific for the recurrent inhibition. Similar long distance effects were observed in recent psychophysiological experiments (Polat and Sagi 1993, Cannon and Fullencamp 1996).

The observation that the effects of the recurrent pathway expand beyond its strict anatomical limits could have also other functional implications. It can contribute to oscillatory phenomena by encompassing larger neuronal assemblies within the LGN as a putative target for synchronous activity. Indeed, the PGN was found to contribute to oscillatory activity at the thalamic level (Steriade et al. 1993).

The nonlinearities reported here are strongly related to a spontaneous activity level. For sufficiently high values of background input B, the overlapping inhibitory surrounds from T and C stimuli may not be strong enough for lowering the cell activity below the zero firing level and producing the threshold effects. Thus increasing the spontaneous activity level in the LGN should decrease the probability of experimental observation of the reported nonlinear RF properties.

A long time ago Maffei and Fiorentini (1972) proposed that the effect of simultaneous contrast which was shown to appear beyond retinal level, could be attributed to geniculate circuitry. Since this effect was observed in larger area then those of individual receptive field they predicted its origin in a convergent network, build up from central areas of several fields. At this time, after the circuitry of the visual thalamus has been studied, it is easier to suggest that the first possible candidate for the cellular origin of contrast effects should be the perigeniculate recurrent network. More recently psychophysiological experiments revealed that the lateral interaction of small stimuli within human area centralis depend in a nonlinear manner on their contrast (Sagi and Hochstein 1985, Cannon and Fullenkamp 1996). These data are in agreement with the prediction of our model which were discussed above.

We know one other model describing nonlinearities generated by RF surround. In his work, Pinter (1985) used the nonlinear character of lateral inhibition to explain the adaptation of spatial modulation transfer function. It is therefore worth to underlie that the only source of nonlinearities discussed in this paper was the threshold mechanism for cell activation. Only these nonlinearities were further propagated through the linear recurrent inhibitory connections.

ACKNOWLEDGEMENTS

We thank Dorota Krakowska and Ewa Kublik, MD, for their excellent help with computer drawings. This work was supported by State Committee for Scientific Research (grant no. 4.P05A.079.09 and statutable to the Nencki Institute).

REFERENCES

Ahlsen G., Lindström S., Lo F. (1983) Excitation of perigeniculate neurones from X and Y principal cells from X and Y principal cells in the lateral geniculate nucleus of the cat. Acta Physiol. Scand. 118: 445-448.

Ahlsen G., Lindström S., Lo F. (1985) Interaction between inhibitory pathways to principal cells in the lateral geniculate body of the cat. Exp. Brain Res. 58: 134-143.

Amit D.J. (1989) Modelling brain function. The world of attractor neural networks. Cambridge University Press, Cambridge, p. 440.

Cannon M.W., Fullencamp S.C. (1996) A model for inhibitory lateral interaction effects in perceived contrast. Vision Res. 36: 1115-1125.

Cleland B.G., Dubin M.W., Levick W.R. (1971) Sustained and transient neurones in the cats retina and lateral geniculate nucleus. J. Physiol. 218: 473-496.

Dubin M.W., Cleland B.G. (1977) Organization of visual inputs to interneurones of lateral geniculate nucleus of the cat. J. Neurophysiol. 40: 410-427.

Enroth-Cugel C., Robson J.G. (1966) The contrast sensitivity of retinal ganglion cells of the cat. J. Physiol. 187: 517-552.

Hoffman K.P., Stone I., Sherman S.M. (1972) Relay of receptive field properties in dorsal lateral geniculate nucleus of the cat. J. Neurophysiol. 95: 518-531.

Hubel D.H., Wiesel T.N. (1961) Integrative action in the cats lateral geniculate body. J. Physiol. 155: 385-398.

Levick W.R., Cleland B.G., Dubin M.W. (1972) Lateral geniculate neurones of cat: retinal input and physiology. Invest. Ophthalmol. 11: 302-311.

Lindström S. (1982) Synaptic organization of inhibitory pathways to principal cells in the lateral geniculate nucleus of the cat. Brain Res. 234: 447-453.

Lindström S., Wróbel A. (1986) Inhibitory circuits of the cat's lateral geniculate nucleus. Structure et function dans le systeme visuel. Colloque INSERM. Lyon. Abstr. p.5.

Lindström S., Wróbel A. (1990) Frequency dependent corticofugal excitation of principal cells in the cat's dorsal lateral geniculate nucleus. Exp. Brain Res. 79: 313-318.

Lehmkule S., Kratz K.E., Mengel S.C., Sherman S.M. (1980) Spatial and temporal sensitivity of X- and Y-cells in d-LGN of the cat. J. Neurophysiol. 43: 520-541.

Maffei L., Fiorentini A. (1972) Retinogeniculate convergence and analysis of contrast. J. Neurophysiol. 35: 65-72.

McCormick D.A. (1992) Neurotransmitter actions in the thalamus and cerebral cortex and their role in neuromodulation of thalamocortical activity. Prog. Neurobiol. 39: 337-388.

Panecki S.J. (1990) Neural network with continuously variable activation level and finite propagation velocity. Abstr. XIII Ann. ENA Meeting, Stockholm 1990: 307.

Peichl L., Wässle H. (1979) Size, scatter and coverage of ganglion cell receptive field centres in the cat retina. J. Physiol. 291: 65-80.

Pinter R.B. (1985) Adaptation of spatial modulation transfer functions via nonlinear lateral inhibition. Biol. Cybern. 51: 2285-291.

Polat U., Sagi D. (1993) Lateral interaction between spatial channels: suppression and facilitation revealed by lateral masking experiments. Vision Res. 33: 993-999.

Rodieck, R.W., Stone, J. (1965) Analysis of receptive fields of cat retinal ganglion cells. J. Neurophysiol. 28: 833.

Sagi D., Hochstein S. (1985) Lateral inhibition between spatially adjacent spatial-frequency channels? Percept. Psychophys. 37: 315-322.

Sherman S.M., Koch C. (1986) The control of retinogeniculate transmission in the mammalian lateral geniculate nucleus. Exp. Brain Res. 63: 1-20.

Smith H.L. (1991) Convergent and oscillatory activation dynamics for cascades of neural nets with nearest neighbour competitive or cooperative interactions. Neural Networks 4: 41-46.

So Y.T., Shapley R.M. (1979) Spatial properties of X and Y cells in the LGN of the cat and conduction velocities of their inputs. Exp. Brain Res. 36: 533-550.

So Y.T., Shapley R.M. (1981) Spatial tuning of cells in and around LGN of the cat: X and Y relay cells and PGN interneurones. J. Neurophysiol. 45: 107-120.

Steriade M., McCormick A., Sejnowski T.J. (1993) Thalamocortical oscillations in the sleeping and aroused brain. Science 262: 679-685.

Stevens J.K., Gerstein G.L. (1976) Spatiotemporal organization of cat LGN cells receptive fields. J. Neurophysiol. 39: 213-238.

Troy J.B. (1982) Spatial contrast sensitivities of X and Y type neurones in the cat's d-LGN. J. Physiol. 344: 399-417.

Tsumoto T., Creutzfeldt O.D., Legendy C.R. (1978) Functional organization of the corticofugal system from visual cortex to lateral geniculate in the cat. Exp. Brain Res. 32: 345-364.

Wróbel A. (1981) Two unit recordings from LGN of the cat. Some inhibitory interactions. Acta Neurobiol. Exp. 41: 467-476.

Wróbel A. (1982) Inhibitory mechanisms within the receptive fields of the lateral geniculate body of the cat. Some inhibitory interactions. Acta Neurobiol. Exp. 41: 467-476.

Wróbel A., Gerstein G.L. (1979) Spatiotemporal summation within cat LGN receptive fields. Neurosci. Lett. Suppl. 3: S297.

Wróbel A., Tarnecki R. (1984) Receptive fields of cat's nonrelay LGN and PGN neurones. Acta Neurobiol. Exp. 44: 289-299.

Received 22 July 1996, accepted 7 October 1996